DESIGN, SYNTHESES AND MOLECULAR MODELING OF NUCLEOSIDE ANALOGS AS ANTI-TOXOPLAMOSIS AGENTS AND UNDERSTANDING THE MECHANISM OF VIRAL RESISTANCE AGAINST CLINICALLY ACTIVE NUCLEOSIDES

by

VIKAS YADAV

(Under the Direction of CHUNG K. CHU)

ABSTRACT

The focus of this thesis is on the combinatorial synthesis of benzylthioinosine analogs as subversive substrates for *Toxoplasma gondii*. And on understanding the molecular basis of viral drug resistance observed in several clinically active nucleosides.

Enantiomerically pure 6-benzylthioinosine analogues were synthesized by combinatorial chemistry from D-ribose in 5 steps. The synthetic methodology of enantiomerically pure analogs of 6-benzylthioinosine was developed by solid-state combinatorial synthesis from D-ribose in 8 steps. Among several analogues synthesized, 6-(4-Cyanobenzylthio)-9-β-D-ribofuranosylpurine and 6-(2,4-Dichlorobenzylthio)-9-β-D-ribofuranosylpurine were found to be active against *Toxoplasma gondii*. Molecular modeling studies were conducted to examine the molecular mechanism of drug resistance conferred by rtN236T mutation, on the efficacy of the clinically active drug, adefovir dipivoxil.

INDEX WORDS: Combinatorial synthesis, *Toxoplasma gondii*, Molecular modeling, HBV, drug resistance, Benzylthioinosine analogs, N236T, Adefovir dipivoxil.

DESIGN, SYNTHESES AND MOLECULAR MODELING OF NUCLEOSIDE ANALOGS AS ANTI-TOXOPLAMOSIS AGENTS AND UNDERSTANDING THE MECHANISM OF VIRAL RESISTANCE AGAINST CLINICALLY ACTIVE NUCLEOSIDES

by

VIKAS YADAV

B. Pharm. Sc., Bombay University, India, 2000

A Thesis Submitted to the Graduate Faculty of The University of Georgia in Partial Fulfillment of the Requirements for the Degree

MASTER OF SCIENCE

ATHENS, GEORGIA

2004

DESIGN, SYNTHESES AND MOLECULAR MODELING OF NUCLEOSIDE ANALOGS AS ANTI-TOXOPLAMOSIS AGENTS AND UNDERSTANDING THE MECHANISM OF VIRAL RESISTANCE AGAINST CLINICALLY ACTIVE NUCLEOSIDES

by

VIKAS YADAV

Major Professor: Chung K Chu

Committee: A. C. Capomacchia
Warren Beach

Electronic Version Approved:

Maureen Grasso
Dean of the Graduate School
The University of Georgia
August 2004

ACKNOWLEDGEMENTS

First of all, I would like to express my sincere appreciation and gradtitude to my major professor Dr. Chung K. Chu for his support, encouragement, and patient guidance. I would like to extend my thanks to Dr. Anthony C. Capomacchia and Dr. Warren Beach for their serving in my advisory committee and continunous support and help.

I also would like to thank the National Institute of Health for the financial support and University of Georgia for giving me a wonderful research environment.

I am also grateful to the labmates, Dr. G. Gumina, Dr. Y. Chong, Dr. H. Choo and Mr. Y. H. Jin for their help and support in my experiments and also to Mrs. W. Nix for her administrative help and support during my graduate study.

TABLE OF CONTENTS

Page

LIST OF TABLES

Page

LIST OF FIGURES

Page

CHAPTER 1

SYNTHESIS, BIOLOGICAL ACTIVITY AND MOLECULAR MODELING OF 6-BENZYLTHIOINOSINE ANALOGUES AS SUBVERSIVE SUBSTRATES OF *TOXOPLASMA GONDII* ADENOSINE

Introduction

Toxoplasma gondii is an intracellular parasitic protozoan belonging to the phylum Apicomplexa. The parasite has a high incidence of infections in humans as well as in warm-blooded animals. Approximately a billion people worldwide are seropositive to *T. gondii*, including more than 60 million people in the United States.[1] Infection with *T. gondii* is asymptomatic unless the host immune system is seriously compromised such as in AIDS, organ transplantation, or unborn children of infected mothers.[2] Toxoplasmosis is the most common and life-threatening infection of the central nervous system,[2,3] and its therapy has not changed in the past three decades. Sulfonamides and pyrimethamine are two drugs widely used to treat toxoplasmosis in humans. Although these drugs are helpful in the acute stage of the disease, usually they do not eradicate infection. Furthermore, in over half of AIDS patients, prolonged exposure to this regimen can induce severe side-effects such as bone marrow suppression and severe skin rashes.[4,5,6] Hence, there is a critical need to develop new and effective drugs with significant low host toxicity.

Rational drug design is usually based on exploitation of biochemical and physiological differences between pathogen and host. One potential target for chemotherapeutic intervention against *T. gondii* is purine metabolism.[6,7] These parasites replicate rapidly and require large amounts of purines for the synthesis of nucleic acids and other vital components.[6-8] However, *T. gondii* is a purine auxotroph and hence must rely on purine salvage from the host.[7] Furthermore, since *T. gondii* can convert adenine to guanine nucleotides, but not the reverse, only salvaged adenine, adenosine, hypoxanthine, or inosine can fulfill all of its purine requirements for nucleic acid synthesis.[6,9] Adenosine is incorporated into the nucleotide pools of *T. gondii* at a 10-fold higher rate than any other purine nucleobase or nucleoside.[6,9] The major route of adenosine metabolism in *T. gondii* is direct phosphorylation to AMP, from which all other purine

nucleotides can be synthesized. This reaction is catalyzed by adenosine kinase (EC.2.7.1.20), which is almost 10 times more active than any other purine salvage enzyme in these parasites.[6] In mammalian cells, adenosine is catabolized to hypoxanthine by the sequential reactions of adenosine deaminase (EC.3.5.4.4) and purine nucleoside phosphorylase (EC.2.4.2.1), respectively.[7,11] Neither of these enzymes have any appreciable activity in *T. gondii.*[6]

T. gondii adenosine kinase has been established as an excellent potential chemotherapeutic target for the treatment of toxoplasmosis.[7,10-12] Structure-activity relationship as well as biochemical, metabolic and molecular studies established that the substrate specificity as well as other characteristics of *T. gondii* adenosine kinase differ significantly from those of the human enzyme.[7,10-12] These studies have also demonstrated that 6-benzylthioinosine (BTI) is a substrate for the parasite, but not the human adenosine kinase.[7,10,11] Furthermore, BTI was shown to be preferentially metabolized to its monophosphorylated form and becomes selectively toxic to *T. gondii* but not their host, thereby acting as a subversive substrate.[7,10,11] BTI and few other members (**6a, 6d, 6g** and **6f**) of this class of compounds have been previously synthesized and tested as inhibitors of nucleoside transport systems in mammalian cells.[13] However, none of these compounds were shown to enter into or be metabolized by uninfected mammalian cells.[7,11-14] In view of the fact that BTI is a substrate for the parasite adenosine kinase (but not the host) and becomes selectively toxic to *T. gondii* [7,10,11], modification of the chemical structure of BTI could further potentiate its anti-toxoplasmic efficacy. Therefore, we focused on optimizing this lead compound by combinatorial synthesis with the aim of designing more potent subversive substrates for the *T. gondii* adenosine kinase. Herein we report the synthesis of a new class of BTI analogues that act as potent and selective subversive substrates for *T. gondii*, but not the human, adenosine kinase.

Results and Discussion

Chemistry

For the synthesis of 6-substituted 9-β-D-ribofuranosylpurine analogues, we chose a straightforward strategy amenable to combinatorial synthesis (Figure 1). The sugar 1-*O*-acetyl-2,3,5-tri-*O*-benzoyl-D-ribofuranose **(1)** was condensed[15] with 6-chloropurine to obtain 6-chloro-9-(2,3,5,-tri-*O*-benzoyl-β-D-ribofuranosyl)-9H-purine **(2)**. Subsequent treatment with methanolic ammonia gave 6-chloro-9-β-D-ribofuranosyl-9H-purine **(3),** which on coupling[16] with trityl chloride resin gave the key intermediate **4**. Nucleophilic displacement with the appropriate thiols[17] led to resin-linked 6-(substituted benzylthio)purine **5**. Cleavage from the resin with 2% trifluoroacetic acid and 5% triisopropylsilane[18] afforded the nearly pure 6-(substituted benzylthio)purines **6** in excellent overall yield.

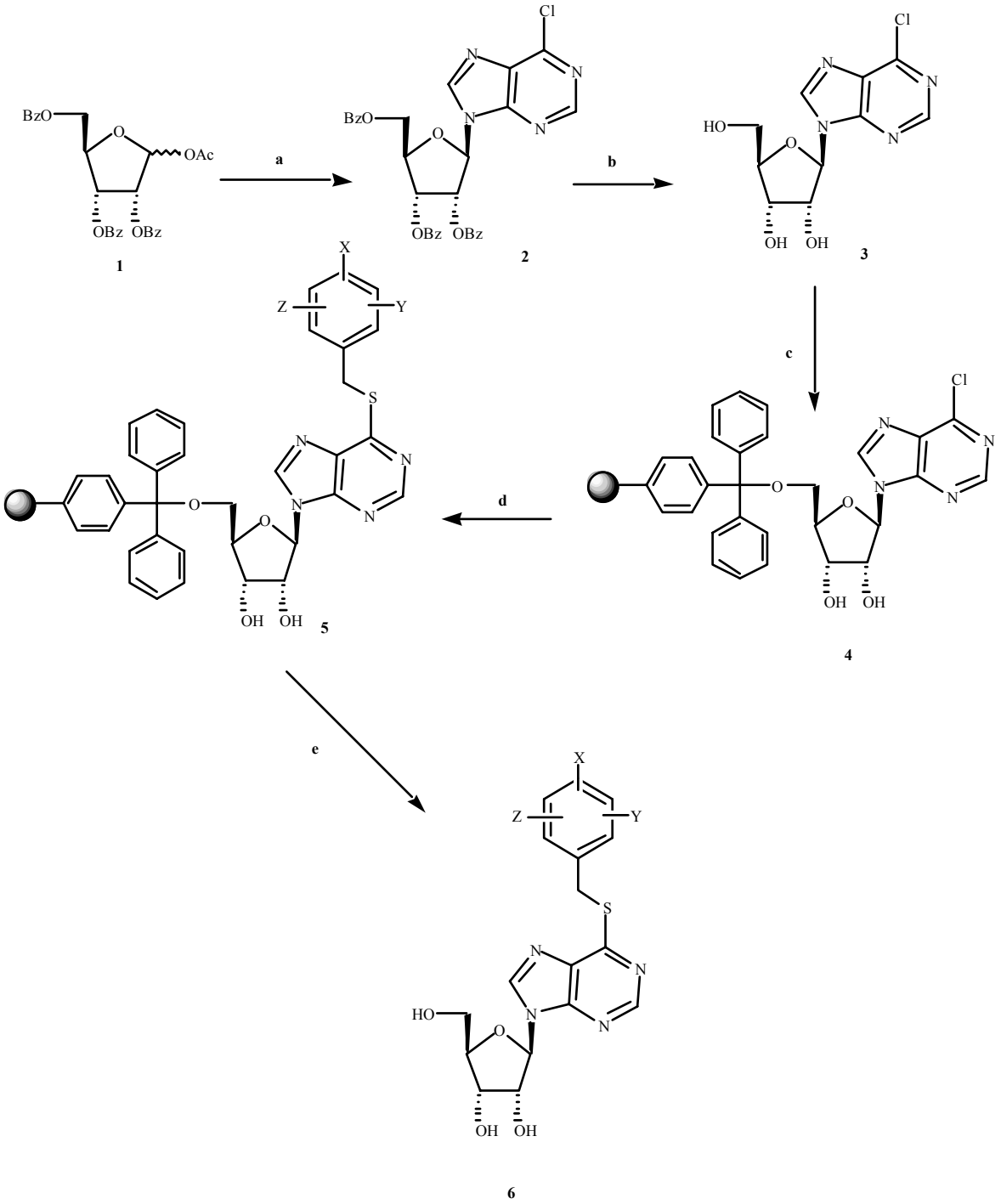

Figure 1.1 Synthesis scheme for 6-benzylthioinosine analogs.

Reagents: (a) 6-chloropurine, hexamethyldisilazane, $(Me)_3SiCl$, $(Me)_3SiTfa$ (b) Methanolic NH_3, Overnight (c) Trityl resin, (anhydrous) Pyridine, 2 days (d) TEA, Substitutedbenzylthiol, 55 °C (e) 2% TFA, 5% TIS, CH_2Cl_2 (anhydrous).

Structure-Activity Relationships. The binding affinities (apparent K_m values) of the newly synthesized BTI analogues to *T. gondii* and human adenosine kinase were evaluated in enzyme based assays. The binding affinity of adenosine and BTI were also evaluated as a reference for the newly synthesized BTI analogues. BTI and its analogues did not bind to the human hepatic enzyme. On the other hand, several BTI analogues were identified as better substrates of the *T. gondii* adenosine kinase than the natural substrate (adenosine). The apparent K_m values of adenosine, BTI and the BTI analogues are reported in Table 1.1.

Table 1.2. Binding affinity (apparent K_m) of substituted 6-benzylthioinosine analogues, 6-benzylthioinosine and adenosine to *Toxoplasma gondii* adenosine kinase.

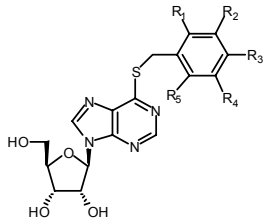

Compound	R_1	R_2	R_3	R_4	R_5	K_m [µM]
6a	CH_3	H	H	H	H	1.5 ± 0.6
6b	F	H	H	H	H	*
6c	Cl	H	H	H	H	1.4 ± 0.2
6d	H	CH_3	H	H	H	1.3 ± 0.6
6e	H	CF_3	H	H	H	2.9 ± 1.3
6f	H	NO_2	H	H	H	3.0 ± 1.6
6g	H	H	CH_3	H	H	3.3 ± 1.1
6h	H	H	OCF_3	H	H	140.7 ± 8.3
6i	H	H	Br	H	H	7.5 ± 2.6
6j	H	H	OCH_3	H	H	2.6 ± 0.4
6k	H	H	*tert* Butyl	H	H	112.8 ± 11.7

6l	H	H	$COOCH_3$	H	H	96.1 ± 1.6
6m	H	H	Cl	H	H	2.1 ± 1.0
6n	H	H	NO_2	H	H	1.1 ± 0.2
6o	H	H	CN	H	H	0.9 ± 0.1
6p	H	H	F	H	H	1.2 ± 0.3
6q	Cl	H	Cl	H	H	0.7 ± 0.2
6r	Cl	H	H	H	F	37.7 ± 2.3
6s	H	Cl	Cl	H	H	2.5 ± 1.3
6t	CH_3	H	CH_3	H	CH_3	149.6 ± 2.7
6-Benzylthioinosine	H	H	H	H	H	2.4 ± 1.2
Adenosine	-	-	-	-	-	2.4 ± 0.2

*Could not be determined

There were no differences in the biological activities of electron-rich and electron-deficient substitution at the *ortho* position, for example, compounds **6a** (CH_3) and **6c** (Cl). At the *meta* position, there seems to be a very slight preference for electron-rich substituents over electron-deficient substituents. However these differences may be within the limits of the experimental error for the biological assay. Substitution at the *para* position provided more significant changes in activity compared to any other position. The *para* position was more amenable to modifications, which seemed to be affected by both the hydrophobicity and the electronegativity of the substituent. In the case of halogens, the increase in the electronegativity of the halogen was accompanied by increased binding to the enzyme (compounds **6i**, **6m** and **6p**). Steric bulk of the substitution at the *para* position appeared to play a critical role in binding. Increasing the bulkiness of substitution decreased the binding drastically (compounds **6k** and **6l)**. In general, electron-deficient substituents were preferred (**6m**, **6n, 6o** and **6p)**. In the case of multiple substitutions, it was noted that substitutions at both the *ortho* and *para* positions (**6q**) were more

favorable than those on *meta* and *para* positions (**6s**). In the case of triple substitutions, the 2,4,6-trimethyl analogue (**6t**) showed drastic loss of activity, whereas a single methyl substitution at the *ortho*, *meta* or *para* positions exhibited appreciable activities (compounds **6a**, **6d** and **6g**).

Anti-Toxoplasmic Activity. The two best substrates, **6o** and **6q**, and the two weakest substrates, **6h** and **6k**, (Table 1.1) were evaluated as potential anti-toxoplasmic agents in cell based assays using wild type (RH) and adenosine kinase deficient ($TgAK^{-3}$) strains of *T. gondii*. As a positive control, pyrimethamine and sulfadiazine, the standard chemotherapeutic agents used in the treatment of toxoplasmosis, were also evaluated. It is evident from Table 1.2 that all the tested compounds, **6o, 6q**, **6h** and **6k**, were effective against infection with the wild type parasites albeit to different degrees. Compounds **6o** and **6q** were more effective than **6h** and **6k.** None of these compounds, however, was effective against infection with the adenosine kinase deficient strain ($TgAK^{-3}$). These results demonstrate that the presence of *T. gondii* adenosine kinase is a requirement for these compounds to exert their anti-toxoplasmic effect. Therefore, these compounds are substrates for *T. gondii* adenosine kinase *in vivo* as was the case with the *in vitro* enzyme assays. It should also be noticed that, the effectiveness of these compounds *in vivo* (Table 1.2) appears to be strongly correlated with their binding affinity (apparent K_m values) to the parasite's adenosine kinase (Table 1.1). Furthermore, Table 1.2 also shows that all four compounds, **6o**, **6q**, **6h** and **6k**, had no toxic sideeffect on the survival of uninfected host cell; indicating that host toxicity is of little concern for these compounds. The lack of host toxicity is due to at least two factors. First, such 6-substituted compounds are not substrates for the human adenosine kinase.[7,10,11] Thus, no toxic nucleotides were formed in the absence of the parasite enzyme. Secondly, the newly synthesized compounds are analogues of *p*-nitrobenzylthioinosine (NBMPR), a known inhibitor of nucleoside transport in mammalian cells, which is not

transported or metabolized by uninfected host cells.[7,11,12] Therefore, the newly synthesized compounds may act as NBMPR and not gain entry to uninfected host cells to exert toxic side-effects. Finally, Table 1.2 shows that the two compounds (**6o** and **6q**) were equivalent or better than sulfadiazine and/or pyrimethamine.

Table 1.3: Effect of different substituted 6-(Substituted benzylthio)purine ribosides analogues, and known therapeutic compounds on percent survival[a] of wild type (RH) and adenosine kinase deficient ($TgAK^{-3}$) strains of *Toxoplasma gondii* grown in human fibroblasts in culture.

Compound	**Infection**	**Concentration [µM]**				
		0	5	10	25	50
6q	Wild Type (RH)	100	94.8	79.1	34.5	0
	$TgAK^{-3}$	100	100	100	100	100
	None[b]	100	98.1	99.2	94.0	99.5
6o	Wild Type (RH)	100	61.5	45.2	7.56	0
	$TgAK^{-3}$	100	100	100	100	100
	None[b]	100	97.4	96.9	100	99.7
6h	Wild Type (RH)	100	93.1	64.9	54.5	44.0
	$TgAK^{-3}$	100	100	100	97.6	95.1
	None	100	100	99.9	97.4	98.6
6k	Wild Type (RH)	100	83.3	71.7	47.2	12.2
	$TgAK^{-3}$	100	100	100	100	99.9
	None	100	99.7	100	99.1	97.1

Sulfadiazine	Wild Type (RH)	100	75.7	64.5	59.2	46.6
	None[b]	100	98.2	99.7	99.8	100
Pyrimethamine	Wild Type (RH)	100	53.8	36.3	11.8	6.9
	None[b]	100	100	98.8	100	100

[a]*Survival of parasites was measured by incorporation of [5,6-^{3}H]uracil as previously described by el Kouni et al. [11].*

[b]*Survival of uninfected human fibroblasts was measured by the MTT method as previously described.[11]*

Molecular Modeling.

Prior to the current studies, preliminary structure activity relationship studies have been performed by el Kouni and co-workers,[10] and from these preliminary studies several *T. gondii* adenosine kinase ligands have been identified, including 7-iodotubercidin[10] which is quite potent, but cytotoxic and a non-selective inhibitor.[19] The X-ray structure 7-iodotubercidin bound to *T. gondii* adenosine kinase has also been reported.[20] The important findings from the detailed study of these reported crystal structures of the complexes coupled with the detailed structure activity relationship analysis were the following: a) 2'-OH and 3'-OH are crucial for binding. b) Two hydrophobic pockets exist, one at the S^6 region and another at N^7 region. c) The size of the hydrophobic pocket is larger at S^6 as compared to that at N^7.

T. gondii adenosine kinase is a 363 residue monomeric protein that catalyzes the transfer of the γ-phosphate group from ATP to adenosine to form ADP and AMP, respectively.[20] The protein consists of two domains: a large domain (α/β) and a small domain (α/β). The substrates and the products are bound at the domain interfaces or the hinge. This binding pocket is sub-

divided into three regions, the ribose binding region, the purine binding region and the hydrophobic region. The ribose binding region is mostly hydrophilic and provides the anchoring of the adenosine in the proper orientation by forming a network of hydrogen bonds with residues Asp24, Gly69 and Asn73. The purine binding region is hydrophobic and also forms hydrogen bonds with the surrounding residues, with most of the binding mediated *via* trapped water molecules. It has been hypothesized[20] that residues Leu46, Leu142, Tyr169 and Phe201 line the putative binding pocket in the *apo* form of the enzyme, and present the hydrophobic surface for the binding of the adenosine. Hence, we propose that this hydrophobic interaction is strengthened when the residues actually move into the pocket and results in hinge bending. During adenosine binding Gly68 and Gly69 side chains undergo conformational changes, causing domain movements and binding pocket formation. And due to these simultaneous movements, there are few extra residues which add up to the initial set of hydrophobic residues to ultimately define the binding pocket (Figure 1.2). Residues Ile22, Ala44, Thr45, Leu46, Leu138, Thr140, Leu142, Tyr169, Thr172, Ala199 and Phe201 along with Leu205 form a cavity that accommodates the purine base. These include the same set of residues, which line the putative binding pocket in the *apo* state and subsequently form the hydrophobic region of the adenosine binding pocket in the complexed structure.

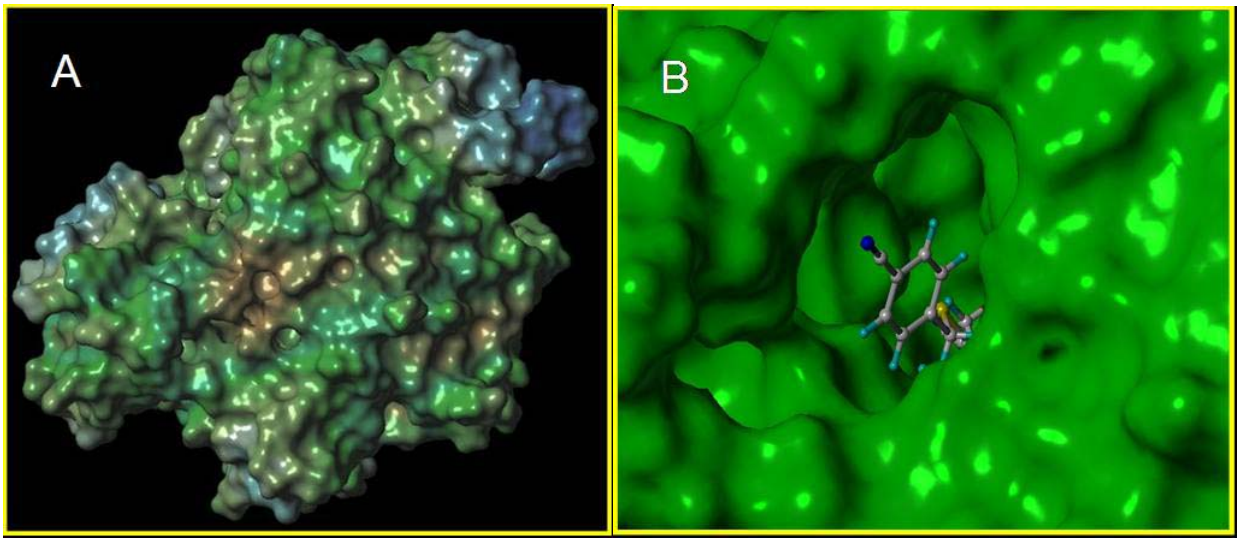

Figure 1.2a. Connolly surface representation of *Toxoplasma gondii* adenosine kinase with its hydrophobic potential mapped on it. Notice the dark brown spot representing the hydrophobic patch on the enzyme surface. This is the hydrophobic region where benzyl substituents of the ligands position themselves. **1.2b.** Docked 6-benzylthioinosine (BTI) analogue in *T. gondii* adenosine kinase.

In our studies, four compounds were selected for docking calculations with the *T. gondii* adenosine kinase. The natural substrate (adenosine), the lead compound (BTI) and the two most active compounds, 6-(4-Cyanobenzylthio)-9-β-D-ribofuranosylpurine (**6o**) and 6-(2,4-Dichlorobenzylthio)-9-β-D-ribofuranosylpurine (**6q**). The lowest energy conformation of various BTI analogues as obtained from the MC/EM studies is shown in Figure 1.3. The MC/EM method predicts the binding mode of the natural substrate adenosine with fairly high accuracy (with RMSD of 0.006Å from the reported crystal structure). In the case of BTI, the benzyl group occupies the hydrophobic region at the S^6 region of the binding pocket in a favorable manner. It is even evident from the superimposition of the 10 low energy conformers that the change in conformation takes place only at the glycosidic bond level or sugar ring, but the overall

orientation of the benzyl group was always in the same region. The orientation of the base is "anti" in all the conformations. The sugar conformation is 2'-endo in all the low energy conformations. In the case of 6-(4-Cyanobenzylthio)-9-β-D-ribofuranosylpurine (**6o**), a similar trend is observed, the benzyl group positions itself in the hydrophobic pocket and the presence of the cyano group at the *para* position, also increases the net van der Waal's interaction with surrounding residues. Here again, as in the case of BTI, the sugar conformation is 2'-endo, which is the preferred conformation of sugar for reactions catalyzed by kinases. In the case of 6-(2,4-Dichlorobenzylthio)-9-β-D-ribofuranosylpurine (**6q**), the position of the benzyl group is not changed, but the net electronegative potential on the phenyl ring is increased. This slight increase is presumably responsible for the enhanced binding of **6q** compared to **6o**. Both, **6q** and **6o** are better substrates than adenosine, which can be attributed to a combination of enhanced hydrophobicity and enhanced electronegative potential. The sugar ring in all the low-energy conformers has the same envelope conformation as that of adenosine during phosphate transfer from ATP.[20] This similarity with the transition state conformation may further add to its better binding ability.

The S^6 hydrophobic region is a long tubular pocket lined with hydrophobic groups. The pocket seems to broaden near its end, where it forms a funnel-like shape. The tubular shape of the pocket can accommodate the phenyl moiety of the benzyl substituent as well as single atom substituents (e.g., halogens) that are electronegative and can form favorable van der Waals interaction with the residues lining the pocket.

The conclusions from our modeling studies are: a) We confirmed that the S^6 benzyl substitution occupies the hydrophobic pocket, and this pattern seems not to be affected by the different substitution pattern on the phenyl ring of the benzyl group; b) the hydrophobic

interactions inside this binding pocket can be increased by increasing the hydrophobicity of the substitution on the phenyl ring, although caution should be exercised in order not to introduce steric hindrance; c) small electron-deficient substituents at the *ortho* and *para* position enhance the binding energy by van der Waals interactions and putative hydrogen bonding, the effect being more pronounced at the *para* position than at the *ortho* position, however here again care should be exercised not to introduce any steric clashes with the side chains of the residues lining the pocket.

In summary, we have designed a novel class of potent and selective anti-toxoplasmosis agents. The basic protocol for the combinatorial synthesis of this class and other related classes of compounds has been developed. We have generated several analogues which are better substrates for *T. gondii* adenosine kinase relative to the natural substrate (adenosine). This enhanced activity can be attributed to the combined effect of hydrophobic as well as van der Waals interactions, as confirmed by molecular modeling studies. The two most potent (**6q** & **6o**) as well as the two weakest (**6h** & **6k**) analogues were tested in cell-based assays and were compared to sulfadiazine and pyrimethamine, the drugs of choice for treatment of toxoplasmosis in terms of their anti-toxoplasmosis activity. In addition, these compounds were devoid of host-toxicity (Table 1.2). To further confirm the potential usefulness of these two compounds, *in vivo* animal efficacy tests are warranted.

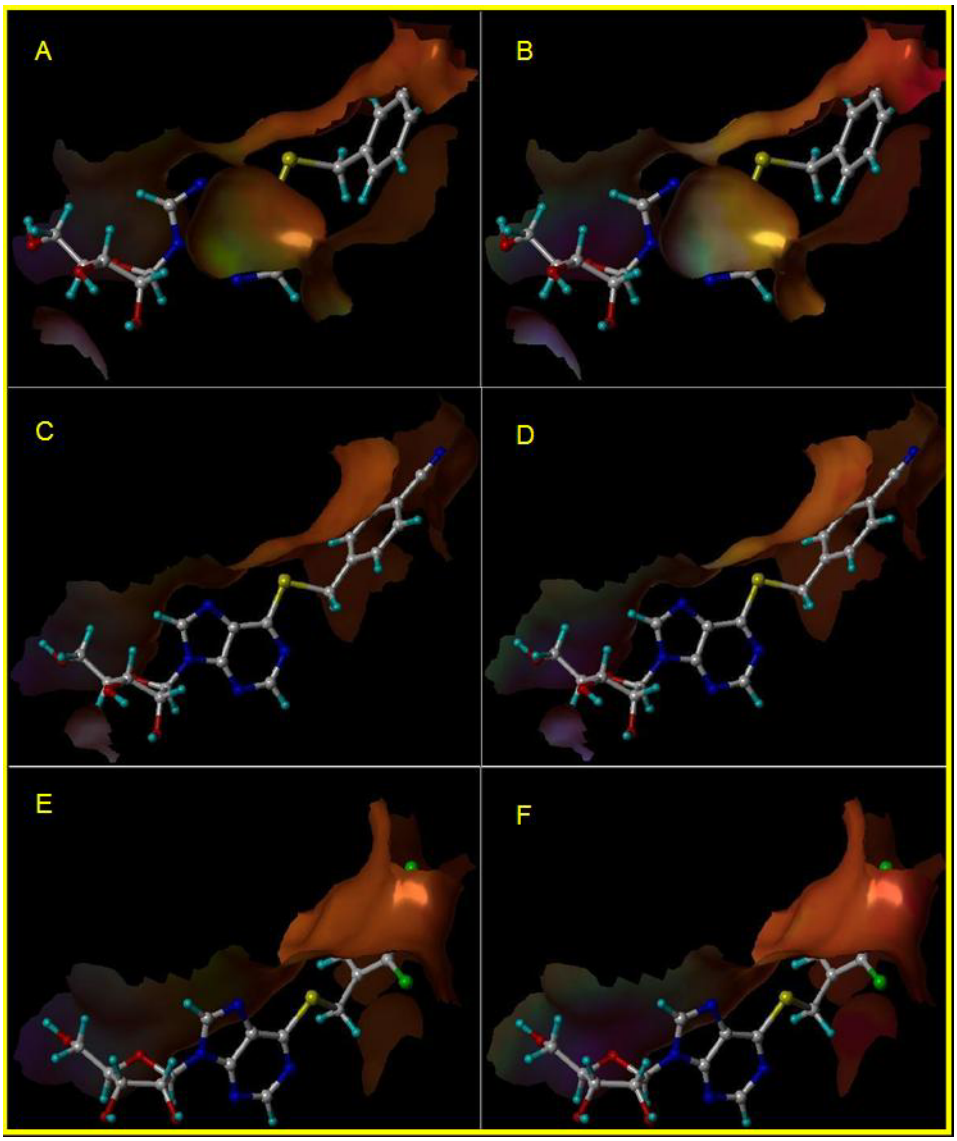

Figure 1.3. Connolly surface representation of the binding mode of 6-benzylthioinosine (BTI) (images A & B), 6-(4-Cyanobenzylthio)-9-β-D-ribofuranosylpurine (**6o**) (images C & D) and 6-(2,4-Dichlorobenzylthio)-9-β-D-ribofuranosylpurine (**6q**) (images E & F) with their hydrophobicity (left column) and electrostatic potential (right column) mapped.

Experimental Section

Solid phase synthesis was performed on Argonaut Quest 210 organic synthesizer. Melting points were determined on a Mel-temp II laboratory device and are uncorrected. NMR spectra were recorded on a Bruker AMX400 MHz Fourier Transform spectrometer; chemical shifts are reported in parts per million(δ) and, signals are quoted as s (singlet), d (doublet), t (triplet), m (multiplet), and dd (double of doublets). UV spectra were obtained on a Beckman DU-650 spectrophotometer. Optical rotations were measured on a JASCO DIP-370 digital polarimeter. TLC was performed on Uniplates (silica gel) purchased from Analtech. Co. and Elemental analysis were performed by Atlantic Microlab Inc., Norcross, GA.

6-Chloro-9-(2, 3, 5,-tri-O-benzoyl-β-D-ribofuranosyl)-9H-purine (2)

6-Chloropurine (2.80 g, 0.018 mol) and **1** (8.38 g, 0.016 mol) were weighed together in a reaction flask and 100 mL of anhydrous acetonitrile was added. To the mixture were added: hexamethyldisilazane (3.48 mL, 0.016 mol), trimethylsilyl chloride (3.15 mL, 0.025 mol) and trimethyl silyl triflate (4.77 mL, 0.025 mol). The mixture was refluxed for 2.5 h, dichloromethane was added and the solution was extracted with sat. $NaHCO_3$ solution. The organic phase was dried over $MgSO_4$ and evaporated. Residue was then purified by column chromatography (Hexane-EtOAc 80:20). Upon concentrating the suitable fractions, it yielded (9.3 g, 94% yield) of **2** as a white lustrous solid. mp = 114 – 115 °C; $[\alpha]^{25}{}_{D}$ –63.772 (c 0.085, $CHCl_3$) ; UV (CH_2Cl_2) λ_{max} 264 nm; ^{1}H NMR ($CDCl_3$): δ = 8.61 (s, 1H); 8.28 (s, 1H); 7.26 – 8.09 (m, 15H); 6.45 (d, 1H, *J*= 4.9 Hz); 6.42 (dd, 1H, *J*= 4.9, 5.5 Hz); 6.25 (dd, 1H, *J*= 5.2, 5.3 Hz); 4.94 (dd, 1H, *J*= 3.3, 12.4 Hz); 4.85 – 4.87 (m, 1H); 4.70 (dd, 1H, *J*= 4.1, 12.4 Hz). ^{13}C NMR ($CDCl_3$): δ = 65.1, 69.3, 70.2, 75.4, 81.6, 128.4, 129.7, 130.5, 132.8, 144.8, 147.9, 152.0, 154.9 and 167.0.

6-Chloro-9-β-D-ribofuranosyl-9H-purine (3)

Compound **2** (10.3 g, 1.1 mmol) was dissolved in methanolic ammonia (100 mL) and the solution was stirred at rt overnight. The products were concentrated under reduced pressure and the residue was purified by short column chromatography on silica gel. The appropriate fractions, eluted with $CHCl_3$-EtOH (95:5 v/v), were combined and evaporated to give the title compound **3** as a white solid. (1.79 g, 36% yield). mp = 161 – 163 °C. ^{1}H NMR (DMSO-d_6) δ 8.97 (s, 1H), 8.84 (s, 1H), 6.06 (d, 1H, *J*=5.1Hz), 5.59 (d, 1H, *J*=5.9Hz), 5.28 (d, 1H, *J*=5.1Hz), 5.12 (t, 1H, *J*=5.5Hz), 4.58 (m, 1H), 4.21 (m, 1H), 4.10 (m, 1H), 3.5-3.8 (m, 2H); ^{13}C NMR (DMSO-d_6) δ =151.8, 151.6, 149.4, 145.8, 131.4, 88.3, 85.8, 74.1, 70.1, 61.0

Resin-coupled 6-chloro-9-β-D-ribofuranosyl-9H-purine (4)

5 g of the trityl resin and 2 g of **(3)** were taken together in a 25 mL round bottom flask. The vessel was purged with nitrogen followed by addition of anhydrous pyridine 15 mL. Proper care should be taken to make the reaction conditions completely anhydrous. The reaction mixture was stirred gently for 2 days. Then resin beads were washed with 4 portions (4 X 15 mL) of pyridine, followed by 3 portions (3 X 15 mL) of ether, completely dried and weighed. The difference in weight, i.e. 1.9 g corresponds to the amount of **(3)** coupled with the resin. This corresponds to 1.33 mmol of **(3)** being loaded per gram of the resin **(4)**.

General procedure for the solid-phase parallel synthesis of 6-(substituted benzylthio)-9-β-D-ribofuranosylpurine analogues

Step I

Compound **4** [363 mg (~100 mg of **3**)] was added to each microfrit-equipped reaction vessel (RV), followed by 10 mL of methanol. The appropriate thiols[16] (0.1 mL) were then added, followed by 1mL of triethylamine (TEA). The reaction mixture was stirred gently (upward

stroke=50%, Time=4 sec) at 55 °C for 5 h. After 5 h, the RV's were drained and the beads were washed successively with 3x10 mL of methanol, methylene chloride and ether, then dried by purging with nitrogen. No analysis was done at this stage.

Step II

Cleavage of 6-(substituted benzylthio)-9-β-D-ribofuranosylpurine analogues from the resin

The 10 RV's containing the dry resin from step I were filled with 10 mL of methylene chloride followed by the addition of 0.5 mL of triisopropylsilane (TIS) and 0.2 mL of trifluoroacetic acid (TFA). The reaction mixture was agitated (upward stroke=50%, Time=2 sec) for the next 10 minutes after which contents of the RV's were transferred to side B of the synthesizer in the corresponding RV's using a transfer cannula. Then 3 mL of ether was added along with satd. $NaHCO_3$ (2 mL) to neutralize the excess TFA, and the organic layer containing the final product transferred to a vial for further work-up. It is important to that the extraction has to be performed immediately in order to prevent difficult purification and loss of yield due to cleavage of glycoside bond. The organic layer was concentrated, and short flash column (5% MeOH: 95% CH_2Cl_2) was used to remove traces of impurities. The average yield was ~94%. The analogues were recrystalized from methanol.

6-(2-Methylbenzylthio)-9-β-D-ribofuranosylpurine (6a)

Crystalline white solid. Yield = 95%; mp 190 – 191 °C; $[\alpha]^{25}_D$ –57.544 (c 0.17, MeOH); UV (H_2O) λ_{max} 292 nm (ε 38600 pH 2), 292 nm (ε 40800 pH 7), 292 nm (ε 39600 pH 11); ^{1}H NMR (CD_3OD): δ = 8.73 (s, 1H); 8.58 (s, 1H); 7.42 (d, 1H, *J*=7.14 Hz); 7.14 (m, 3H); 6.08 (d, 1H, *J*=5.76 Hz); 4.72 (t, 1H, *J*=5.6 Hz); 4.70 (s, 2H); 4.33 – 4.35 (m, 1H); 4.14 – 4.16 (m, 1H); 3.88 (dd, 1H, *J*=2.74, 12.37 Hz); 3.76 (dd, 1H, *J*=3.0, 12.46 Hz); 2.42 (s, 3H). Anal. ($C_{18}H_{20}N_4O_4S$): C, H, N, S.

6-(2-Fluorobenzylthio)-9-β-D-ribofuranosylpurine (6b)

Crystalline white solid. Yield = 94%; mp 62 – 64 °C; $[\alpha]^{25}_{D}$ –51.761 (c 0.29, MeOH); UV (H_2O) λ_{max} 290.5 nm (ε 36000 pH 2), 290 nm (ε 39700 pH 7), 290.5 nm (ε 38600 pH 11); ^{1}H NMR (CD_3OD): δ = 8.73 (s, 1H); 8.59 (s, 1H); 7.56 (td, 1H, *J*=1.57, 7.68 Hz); 7.24 – 7.30 (m, 1H); 7.06 – 7.11 (m, 2H); 6.07 (d, 1H, *J*=5.7 Hz); 4.7 – 4.72 (m, 3H); 4.33 – 4.35 (m, 1H); 4.14 – 4.16 (m, 1H); 3.88 (dd, 1H, *J*=2.82, 12.36 Hz); 3.76 (dd, 1H, *J*=3.09, 12.37 Hz). Anal. ($C_{17}H_{17}FN_4O_4S$): C, H, N, S.

6-(2-Chlorobenzylthio)-9-β-D-ribofuranosylpurine (6c)

Crystalline white solid. Yield = 97%; mp 208 – 210 °C; $[\alpha]^{25}_{D}$ –44.883 (c 0.10, MeOH); UV (H_2O) λ_{max} 290.5 nm (ε 35900 pH 2), 291 nm (ε 34400 pH 7), 290.5 nm (ε 40900 pH 11); ^{1}H NMR (CD_3OD): δ = 8.74 (s, 1H); 8.59 (s, 1H); 7.64 – 7.66 (m, 1H); 7.40 – 7.42 (m, 1H); 7.21 – 7.27 (m, 2H); 6.07 (d, 1H, *J*=5.65 Hz); 4.80 (s, 2H); 4.71 (t, 1H, *J*=5.36); 4.33 – 4.35 (m, 1H); 4.13 – 4.15 (m, 1H); 3.88 (dd, 1H, *J*=2.90, 12.51 Hz); 3.75 (dd, 1H, *J*=3.0, 12.19 Hz). Anal. ($C_{17}H_{17}ClN_4O_4S$): C, H, N, S.

6-(3-Methylbenzylthio)-9-β-D-ribofuranosylpurine (6d)

Crystalline white solid. Yield = 93%; mp 177 – 179 °C; $[\alpha]^{25}_{D}$ –58.507 (c 0.13, MeOH); UV (H_2O) λ_{max} 292 nm (ε 32800 pH 2), 292 nm (ε 31600 pH 7), 291.5 nm (ε 32900 pH 11); ^{1}H NMR (CD_3OD): δ = 8.71 (s, 1H); 8.59 (s, 1H); 7.22 – 7.26 (m, 2H); 7.16 (t, 1H, *J*=7.46 Hz); 7.05 (d, 2H, *J*=6.38 Hz); 6.07 (d, 1H, *J*=5.7 Hz); 4.72 (t, 1H, *J*=5.65 Hz); 4.63 (s, 2H,); 4.33 – 4.35 (m, 1H); 4.13 – 4.16 (m, 1H); 3.88 (dd, 1H, *J*=2.89, 12.53 Hz); 3.75 (dd, 1H, *J*=2.69, 12.42 Hz); 2.29 (s, 3H). Anal. ($C_{18}H_{20}N_4O_4S$): C, H, N, S.

6-(3-Trifluoromethylbenzylthio)-9-β-D-ribofuranosylpurine (6e)

Crystalline white solid. Yield = 91%; mp 178 – 180 °C; $[\alpha]^{25}_{D}$ –42.611 (c 0.16, MeOH); UV (H_2O) λ_{max} 290.5 nm (ε 34900 pH 2), 290.5 nm (ε 33600 pH 7), 290.5 nm (ε 37000 pH 11); ^{1}H NMR (CD_3OD): δ = 8.72 (s, 1H); 8.60 (s, 1H); 7.80 (s, 1H); 7.75 (d, 1H, *J*=7.23 Hz); 7.46 – 7.53 (m, 2H); 6.07 (d, 1H, *J*=5.7 Hz); 4.75 (s, 2H); 4.71 (t, 1H, *J*=5.39 Hz); 4.33 – 4.35 (m, 1H); 4.13 – 4.16 (m, 1H); 3.88 (dd, 1H, *J*=2.85, 12.40 Hz); 3.76 (dd, 1H, *J*=3.13, 12.38 Hz). Anal. ($C_{18}H_{17}F_3N_4O_4S$): C, H, N, S.

6-(3-Nitrobenzylthio)-9-β-D-ribofuranosylpurine (6f)

Crystalline white solid. Yield = 95%; mp 164 – 166 °C; $[\alpha]^{25}_{D}$ –42.713 (c 0.14, MeOH); UV (H_2O) λ_{max} 286 nm (ε 44100 pH 2), 286 nm (ε 41800 pH 7), 286 nm (ε 39900 pH 11); ^{1}H NMR (CD_3OD): δ = 8.73 (s, 1H); 8.61 (s, 1H); 8.40 (s, 1H); 8.09 (d, 1H, *J*=8.0 Hz); 7.9 (d, 1H, *J*=7.32 Hz); 7.53 (t, 1H, *J*=7.94 Hz); 6.07 (d, 1H, *J*=5.6 Hz); 4.78 (s, 2H); 4.70 (t, 1H, *J*=5.37 Hz); 4.34 (t, 1H, *J*=3.59 Hz); 4.15 (d, 1H, *J*=2.97 Hz); 3.88 (dd, 1H, *J*=2.75, 12.48 Hz); 3.75 (dd, 1H, *J*=2.98, 12.32 Hz). Anal. ($C_{17}H_{17}N_5O_6S$): C, H, N, S.

6-(4-Methylbenzylthio)-9-β-D-ribofuranosylpurine (6g)

Crystalline white solid. Yield = 94%; mp 110 – 112 °C; $[\alpha]^{25}_{D}$ –56.432 (c 0.37, MeOH); UV (H_2O) λ_{max} 292.5 nm (ε 32300 pH 2), 292.5 nm (ε 31100 pH 7), 292 nm (ε 30200 pH 11); ^{1}H NMR (CD_3OD): δ = 8.70 (s, 1H); 8.58 (s, 1H); 7.32 (d, 2H, *J*=6.98 Hz); 7.1 (d, 2H, *J*=6.92 Hz); 6.07 (d, 1H, *J*=5.59 Hz); 4.71 (t, 1H, *J*=5.36 Hz); 4.62 (s, 2H,); 4.33 – 4.35 (m, 1H); 4.13 – 4.16 (m, 1H); 3.88 (dd, 1H, *J*=2.8, 12.3 Hz); 3.76 (dd, 1H, *J*=3.0, 12.36 Hz); 2.29 (s, 3H). Anal. ($C_{18}H_{20}N_4O_4S$): C, H, N, S.

6-(4-Trifluoromethoxybenzylthio)-9-β-D-ribofuranosylpurine (6h)

Crystalline white solid. Yield = 91%; mp 130 – 132 °C; $[\alpha]^{25}_{D}$ –54.081 (c 0.19, MeOH); UV (H_2O) λ_{max} 290.5 nm (ε 14300 pH 2), 290.5 nm (ε 16000 pH 7), 291 nm (ε 16400 pH 11); ^{1}H NMR (CD_3OD): δ = 8.71 (s, 1H); 8.59 (s, 1H); 7.57 (d, 2H, *J*=8.27 Hz); 7.19 (d, 2H, *J*=7.64 Hz); 6.07 (d, 1H, *J*=5.36 Hz); 4.69 – 4.72 (m, 3H); 4.33 – 4.35 (m, 1H); 4.13 – 4.16 (m, 1H); 3.88 (dd, 1H, *J*=2.6, 12.15 Hz); 3.76 (dd, 1H, *J*=2.47, 12.27 Hz). Anal. ($C_{18}H_{17}F_3N_4O_5S$): C, H, N, S

6-(4-Bromobenzylthio)-9-β-D-ribofuranosylpurine (6i)

Crystalline white solid. Yield = 97%; mp 156 – 158 °C; $[\alpha]^{25}_{D}$ –48.688 (c 0.23, MeOH); UV (H_2O) λ_{max} 291.5 nm (ε 28700 pH 2), 291.5 nm (ε 11800 pH 7), 291.5 nm (ε 17900 pH 11);^{1}H NMR (CD_3OD): δ = 8.71 (s, 1H); 8.59 (s, 1H); 7.38 – 7.44 (m, 4H); 6.07 (d, 1H, *J*=5.75 Hz); 4.71 (t, 1H, *J*=5.38 Hz); 4.64 (s, 2H); 4.33 – 4.35 (m, 1H); 4.13 – 4.16 (m,1H); 3.88 (dd, 1H, *J*=2.8, 12.39 Hz); 3.75 (dd, 1H, *J*=3.08, 12.37 Hz). Anal. ($C_{17}H_{17}BrN_4O_4S$): C, H, N, S

6-(4-Methoxybenzylthio)-9-β-D-ribofuranosylpurine (6j)

Crystalline white solid. Yield = 93%; mp 102 - 104 °C; $[\alpha]^{25}_{D}$ –50.844 (c 0.43, MeOH); UV (H_2O) λ_{max} 292.5 nm (ε 32800 pH 2), 292.5 nm (ε 31600 pH 7), 292 nm (ε 31100 pH 11); ^{1}H NMR (CD_3OD): δ = 8.71 (s, 1H); 8.58 (s, 1H); 7.36 (d, 2H, *J*=8.6 Hz); 6.84 (d, 2H, J=8.65 Hz); 6.07 (d, 1H, *J*=5.77 Hz); 4.71 (t, 1H, *J*=5.40 Hz); 4.62 (s, 2H); 4.33 – 4.35 (m, 1H); 4.13 – 4.16 (m,1H); 3.88 (dd, 1H, *J*=2.73, 12.43 Hz); 3.74 – 3.77 (m, 4H). Anal. ($C_{18}H_{20}N_4O_5S$): C, H, N, S

6-(4-*tert*-Butylbenzylthio)-9-β-D-ribofuranosylpurine (6k)

Crystalline white solid. Yield = 92%; mp 74 - 76 °C; $[\alpha]^{25}_{D}$ –43.770 (c 0.16, MeOH); UV (H_2O) λ_{max} 292.5 nm (ε 29400 pH 2), 292.5 nm (ε 29800 pH 7), 292.5 nm (ε 31700 pH 11); ^{1}H NMR

(CD_3OD): δ = 8.71 (s, 1H); 8.58 (s, 1H); 7.31 – 7.38 (m, 4H); 6.07 (d, 1H, *J*=5.76 Hz); 4.72 (t, 1H, *J*=5.41 Hz); 4.64 (s, 2H); 4.33 – 4.35 (m, 1H); 4.14 – 4.16 (m,1H); 3.88 (dd, 1H, *J*=2.77, 12.35 Hz); 3.76 (dd, 1H, *J*=2.77, 12.40 Hz); 1.28 (s, 9H). Anal. ($C_{21}H_{26}N_4O_4S$): C, H, N, S

6-(4-Acetoxybenzylthio)-9-β-D-ribofuranosylpurine (6l)

Crystalline white solid. Yield = 93%; mp 178 - 180 °C; $[\alpha]^{25}_D$ –61.260 (c 0.18, MeOH); UV (H_2O) λ_{max} 291 nm (ε 8000 pH 2), 290.5 nm (ε 11500 pH 7), 285 nm (ε 16600pH 11); ^{1}H NMR (CD_3OD): δ = 8.72 (s, 1H); 8.60 (s, 1H); 7.94 (d, 2H, *J*=8.07 Hz); 7.59 (d, 2H, *J*=8.17 Hz); 6.07 (d, 1H, *J*=5.68 Hz); 4.74 (s, 2H); 4.71 (t, 1H, *J*=5.18 Hz); 4.33 – 4.35 (m, 1H); 4.13 – 4.16 (m,1H); 3.86 - 3.88 (m, 4H); 3.76 (dd, 1H, *J*=3.0, 12.59 Hz). Anal. ($C_{19}H_{20}N_4O_6S$): C, H, N, S

6-(4-Chlorobenzylthio)-9-β-D-ribofuranosylpurine (6m)

Crystalline white solid. Yield = 96%; mp 134 - 136 °C; $[\alpha]^{25}_D$ –52.053 (c 0.26, MeOH); UV (H_2O) λ_{max} 291 nm (ε 24700 pH 2), 291 nm (ε 16900 pH 7), 291 nm (ε 16700 pH 11); ^{1}H NMR (CD_3OD): δ = 8.72 (s, 1H); 8.60 (s, 1H); 7.44 – 7.47 (m, 2H); 7.27 – 7.29 (m, 2H); 6.07 (d, 1H, *J*=5.75 Hz); 4.71 (t, 1H, *J*=5.41 Hz); 4.66 (s, 2H); 4.33 – 4.35 (m, 1H); 4.13 – 4.16 (m,1H); 3.88 (dd, 1H, *J*= 2.85, 12.40 Hz); 3.76 (dd, 1H, *J*=3.13, 12.38 Hz). Anal. ($C_{17}H_{17}ClN_4O_4S$): C, H, N, S

6-(4-Nitrobenzylthio)-9-β-D-ribofuranosylpurine (6n)

Crystalline white solid. Yield = 94%; mp 197 - 198 °C; $[\alpha]^{25}_D$ –58.152 (c 0.21, MeOH); UV (H_2O) λ_{max} 290 nm (ε 38500 pH 2), 289 nm (ε 40300 pH 7), 289 nm (ε 42700 pH 11); ^{1}H NMR (CD_3OD): δ = 8.72 (s, 1H); 8.61 (s, 1H); 8.16 (d, 2H, *J*=8.76 Hz); 7.73 (d, 2H, *J*=8.64); 6.07 (d, 1H, *J*=5.64 Hz); 4.79 (s, 2H); 4.70 (t, 1H, *J*=5.38 Hz); 4.33 – 4.35 (m, 1H); 4.13 – 4.16 (m,1H); 3.88 (dd, 1H, *J*= 2.72, 12.53 Hz); 3.75 (dd, 1H, *J*=3.12, 12.33 Hz). Anal. ($C_{17}H_{17}N_5O_6S$): C, H, N, S

6-(4-Cyanobenzylthio)-9-β-D-ribofuranosylpurine (6o)

Crystalline white solid. Yield = 93%; mp 72 - 74 °C; $[\alpha]^{25}{}_{D}$ –49.651 (c 0.22, MeOH); UV (H_2O) λ_{max} 290.5 nm (ε 48400 pH 2), 290.5 nm (ε 32100 pH 7), 290.5 nm (ε 47400 pH 11); ^{1}H NMR (CD_3OD): δ = 8.71 (d, 1H, *J*=1.52 Hz); 8.60 (d, 1H, *J*=1.38 Hz); 7.63 – 7.68 (m, 4H); 6.07 (d, 1H, *J*=5.67 Hz); 4.73 (s, 2H); 4.70 (t, 1H, *J*=5.08 Hz); 4.33 – 4.35 (m, 1H); 4.13 – 4.15 (m,1H); 3.88 (dd, 1H, *J*= 1.82, 12.32 Hz); 3.75 (dd, 1H, *J*=1.62, 12.28 Hz). Anal. ($C_{18}H_{17}N_5O_4S$): C, H, N, S

6-(4-Fluorobenzylthio)-9-β-D-ribofuranosylpurine (6p)

Crystalline white solid. Yield = 96%; mp 70 - 72 °C; $[\alpha]^{25}{}_{D}$ –52.178 (c 0.18, MeOH); UV (H_2O) λ_{max} 291.5 nm (ε 38100 pH 2), 291.5 nm (ε 37700 pH 7), 291.5 nm (ε 39000 pH 11); ^{1}H NMR (CD_3OD): δ = 8.72 (s, 1H); 8.59 (s, 1H); 7.48 (m, 2H); 7.01(m, 2H); 6.07 (d, 1H, *J*=5.73 Hz); 4.71 (t, 1H, *J*=5.37 Hz); 4.66 (s, 2H); 4.33 – 4.35 (m, 1H); 4.14 – 4.15 (m,1H); 3.88 (dd, 1H, *J*= 2.84, 12.36 Hz); 3.76 (dd, 1H, *J*=3.06, 12.41 Hz). Anal. ($C_{17}H_{17}FN_4O_4S$): C, H, N, S

6-(2,4-Dichlorobenzylthio)-9-β-D-ribofuranosylpurine (6q)

Crystalline white solid. Yield = 97%; mp 190 °C; $[\alpha]^{25}{}_{D}$ –47.024 (c 0.14, MeOH); UV (H_2O) λ_{max} 284.5 nm (ε 10100 pH 2), 284.5 nm (ε 9200 pH 7), 284.5 nm (ε 11500 pH 11); ^{1}H NMR (CD_3OD): δ = 8.74 (s, 1H); 8.60 (s, 1H); 7.67 (d, 1H, *J*=8.31 Hz); 7.48 (d, 1H, *J*=2.04 Hz), 7.26 (dd, 1H, *J*=2.08, 8.31 Hz); 6.07 (d, 1H, *J*=5.68 Hz); 4.77 (s, 2H); 4.71 (t, 1H, *J*=5.26 Hz); 4.33 – 4.35 (m, 1H); 4.14 – 4.16 (m,1H); 3.88 (dd, 1H, *J*= 2.76, 12.35 Hz); 3.76 (dd, 1H, *J*=3.06, 12.40 Hz). Anal. ($C_{17}H_{16}Cl_2N_4O_4S$): C, H, N, S

6-(2-Chloro-6-fluorobenzylthio)-9-β-D-ribofuranosylpurine (6r)

Crystalline white solid. Yield = 94%; mp 102 - 104 °C; $[\alpha]^{25}_{D}$ –55.583 (c 0.18, MeOH); UV (H_2O) λ_{max} 290.5 nm (ε 38500 pH 2), 290.5 nm (ε 37400 pH 7), 290.5 nm (ε 38800 pH 11); ^{1}H NMR (CD_3OD): δ = 8.76 (s, 1H); 8.60 (s, 1H); 7.28 – 7.35 (m, 2H); 7.9 – 7.14 (m, 1H); 6.09 (d, 1H, *J*=5.64 Hz); 4.87 (s, 2H); 4.72 (t, 1H, *J*=5.43 Hz); 4.33 – 4.35 (m, 1H); 4.13 – 4.16 (m,1H); 3.89 (dd, 1H, *J*= 2.50, 12.15 Hz); 3.76 (dd, 1H, *J*=2.91, 12.42 Hz). Anal. ($C_{17}H_{16}FClN_4O_4S$): C, H, N, S

6-(3,4-Dichlorobenzylthio)-9-β-D-ribofuranosylpurine (6s)

Crystalline white solid. Yield = 95%;mp 144 - 146 °C; $[\alpha]^{25}_{D}$ –53.048 (c 0.25, MeOH); UV (H_2O) λ_{max} 290.5 nm (ε 38300 pH 2), 290.5 nm (ε 35500 pH 7), 290.5 nm (ε 32200 pH 11); ^{1}H NMR (CD_3OD): δ = 8.72 (s, 1H); 8.60 (s, 1H); 7.65 (s, 1H); 7.42 (s, 2H); 6.07 (d, 1H, *J*=5.64 Hz); 4.71 (t, 1H, *J*=5.28 Hz); 4.64 (s, 2H); 4.34 (t, 1H, *J*=4.01 Hz); 4.15 (d,1H, *J*=2.97 Hz); 3.88 (dd, 1H, *J*= 2.74, 12.44 Hz); 3.76 (dd, 1H, *J*=2.98, 12.27 Hz). Anal. ($C_{17}H_{16}Cl_2N_4O_4S$): C, H, N, S

6-(2,4,6-Trimethylbenzylthio)-9-β-D-ribofuranosylpurine (6t)

Crystalline white solid. Yield = 93%; mp 184 - 186 °C; $[\alpha]^{25}_{D}$ –67.906 (c 0.20, MeOH); UV (H_2O) λ_{max} 293 nm (ε 41300 pH 2), 293 nm (ε 39600 pH 7), 293 nm (ε 42000 pH 11); ^{1}H NMR (CD_3OD): δ = 8.74 (s, 1H); 8.59 (s, 1H); 6.87 (s, 2H), 6.08 (d, 1h, *J*=5.73 Hz); 4.73 (t, 1H, *J*=5.41 Hz); 4.70 (s, 2H); 4.33 – 4.35 (m, 1H); 4.13 - 4.16 (m,1H); 3.89 (dd, 1H, *J*= 2.75, 12.41 Hz); 3.76 (dd, 1H, *J*=2.99, 12.44 Hz); 2.36 (s, 6H); 2.24 (s, 3H). Anal. ($C_{20}H_{24}N_4O_4S$): C, H, N, S

Molecular Modeling Study. *T. gondii* adenosine kinase functions by induced fit mechanism and involves hinge bending motion of two domains. This domain movement is complex, and

apparently involves further tuning of the protein structure when ATP binds to its region in this pocket. As a result, our initial modeling attempts to use the apo form (1LIO.pdb)[20] of the enzyme were far less successful than subsequent analysis using the full *T. gondii* adenosine kinase–adenosine complex[20] (1LII.pdb). The crystal coordinates of the reported enzyme-inhibitor complex were missing the residues 1–10, 239–240, 255–269 and 359–363. Residues 239–240 and 255–269 were added using the SYBYL Biopolymer module (Tripos Associates, St. Louis, MO). The terminal residues were not added because it has been shown in mutational and sequence deletion studies that their effect on the overall binding affinity was negligible.[20b] We included in our calculations the magnesium and chlorine ions as observed in the crystal structure. The determination of the binding mode of BTI analogues was complicated by the fact that the enzyme functions via an induced-fit mechanism and that only two substrate–enzyme complexes are known, one with the natural substrate adenosine and the other with 7-iodotubericidin. Neither of these enzyme complexes was ideal for these studies, because our analogues are almost ~16Å in length diagonally, whereas the diagonal length of the adenosine and 7-iodotubericidin is ~8Å. In order to determine the binding mode of the BTI analogues, we tested several modeling techniques that had been previously used for enzymes that function by an induced-fit mechanism. We tried Low Mode Conformational Search (LMOD), Monte Carlo Multiple Minimum/Energy Minimization (MCMM/EM), and Monte Carlo/Energy Minimization (MC/EM). Of these methods, only MC/EM was able to reproduce the crystal structure to a fairly good accuracy and has already been used for enzymes of the induced-fit type.[21-23]

All the calculations were performed on MACROMODEL 7.0 (Schrödinger Inc.) with the GB/SA continuum water solvation model. MMFF94s force field, as implemented in MACROMODEL 7.0 was used. In the case of BTI and BTI analogues the starting conformation

was obtained after performing a 50,000 step Monte Carlo conformational search in the GB/SA continuum water solvation model. Ligands were introduced into the binding pocket in a random orientation (in some trial runs they were in entirely opposite orientations). The MOLS command in BATCHMIN was used to translate the molecule along with torsional variation and the Monte Carlo conformational search with search option set to "Usage Directed" was initiated, with Polak-Ribiere 1st derivative Conjugate Gradient (PRCG) as a method for the subsequent energy minimization. The whole enzyme was used in the Energy minimization step. From our experience, no major computational advantage was achieved when only the residues within the 7Å radii of the ligand were used. EM calculations were performed for 500 steps or until the energy difference between subsequent structures was 0.05 Kj/mol. All the torsional angles were allowed to be varied during the search. A Total of 1000 conformations were generated during the MC/EM search. The calculations were very computationally intensive. For example, it required 29 ca. 29 days on R10000 Octane 2 SGI running IRIX 6.5 to perform a 1000 conformations search for a single ligand.

Enzyme Assays

Purified recombinant *T. gondii* adenosine kinase and human liver cytosol[11] were used in these experiments as the source for the parasite and host enzymes, respectively.

Overexpression of *T. gondii* adenosine kinase. The coding sequence of cloned *T. gondii* adenosine kinase gene *TgAK*[24] was PCR amplified and engineered into *Escherichia coli* expression vector pET21a. The coding sequence was verified by DNA sequencing. The resulting plasmid pETgAK was transformed into strain BL21(DE3)plysS competent *E. coli* cells. For the expression of adenosine kinase, cells were grown at 37°C in LB medium (pH 7.5) containing 50 μg/mL of ampicillin, 34 μg/mL of chloramphenicol and 1% glucose. When the OD_{600} reached

0.6, IPTG was added to a final concentration of 1 mM and the incubation was continued for 3 hr. The cells were then harvested by centrifugation at 6500 x g for 15 min at 4°C. The cells were resuspended in 250 mL of cold 20 mM Tris-Cl pH 8.0, followed by centrifugation. The supernatant was removed and the pellet was stored at –70°C. The frozen pellet was resuspended in 20 mL of lysis buffer and sonicated. The suspension was recentrifuged at 33,000 x g for 30 min at 4°C. The total protein concentration of the supernatant was determined by the Bradford method[25] and glycerol was added to a final concentration of 20% and stored at –20°C.

Purification of the recombinant enzyme. The enzyme was purified to apparent homogeneity with a specific activity of 0.9 mmol/min/mg protein and a yield of 5 mg of soluble protein/L of culture by the following method. Aliquots of supernatant collected above were loaded onto a 95 mL Q-Sepharose Fast Flow column (Pharmacia) equilibrated with Buffer A (50 mM Tris-Cl (pH 8.0), 1 mM DTT). The column was then washed with 5 column volumes of Buffer A and eluted with a 10 column volumes linear gradient from 0-1M NaCl in Buffer A at a flow rate of 5.0 mL/min. Fractions of 17 mL were collected. Adenosine kinase eluted as a broad peak at approximately 90-100 mM NaCl. The fractions containing the activity were concentrated, resuspended in Buffer A and reloaded in a 53 mL Q-Sepharose HP26/10 column (Pharmacia) equilibrated in the same buffer. The column was washed with 2 column volume Buffer A and eluted with 20 column volume of a linear gradient 0-300 mM NaCl and 10 mL fractions were collected. Adenosine kinase eluted as a sharp peak at approximately 100 mM NaCl. Fractions containing the activity were pooled, concentrated, resuspended in Buffer A and kept at –75°C. The identity and homogeneity of the purified enzyme was established by N-terminal amino acid sequencing and SDS polyacrylamide gel electrophoresis as a single band at ~49 KD, respectively. The enzyme is stable under these conditions for months.

Evaluation of 6a – 6t as alternative substrates for purified *T. gondii* adenosine kinase. Enzyme assays were run under conditions where activity was linear with time and enzyme concentration.[10,11] Adenosine kinase activity was determined by following the formation of radiolabeled AMP from adenosine. The assay mixture contains 50 mM Tris-Cl, pH 7.4; 2.5 mM ATP, 5 mM $MgCl_2$, 5 mM creatine phosphate, creatine kinase, 5 μM [8-^{14}C]adenosine (55 Ci/mol), 50 μL enzyme in a final volume of 100 μL, in the absence or presence of various concentrations of the compound under evaluation. Incubation was carried out at 37°C and terminated by boiling in a water bath for 2 min followed by freezing for at least 20 min. Precipitated proteins were removed by centrifugation and 10 μL of the supernatant was spotted on silica gel TLC plates. The TLC plates were developed in a mixture of chloroform/methanol/acetic acid (102:12:6 v/v/v). The R_f values were: adenosine, 0.27; adenine, 0.36; AMP, 0.17. The amounts of radioactivity in both the substrate and product(s) were calculated on a percentage basis using a computerized Berthold LB-284 Automatic TLC-Linear Analyzers (Wallac Inc., Gaithersburg, MD). Apparent K_i values of these analogues were calculated from Dixon plots 1/v vs. [I] by least-squares fitting by computer programs developed by Dr. Naguib as previously described.[10,11] Since these compounds are competitive alternate substrates of *T. gondii* adenosine kinase, their apparent K_i values are equal to their apparent K_m value [26] as presented in Table 1.1.

Evaluation of 6-(Substituted benzylthio)purine Ribosides Analogues as Potential Anti-toxoplasmosis Agents Against Tachyzoites in Tissue Culture.

The wild type RH and the adenosine kinase deficient mutant TgAK^{-3} [24] strains of *T. gondii* were used in these experiments. The adenosine kinase deficient mutant TgAK^{-3} was used as a control to verify that the active drugs were metabolized by adenosine kinase *in vivo*. The effects of

purine analogues as anti-toxoplasmosis agents in tissue culture was measured by their ability to inhibit the replication of intracellular *T. gondii* in tissue culture using monolayers of human foreskin fibroblasts (grown for no more than 30 passages) in RPMI 1640 medium.[11,12] The viability of intracellular parasites was evaluated by the selective incorporation of radiolabeled uracil into nucleic acids of the parasites at least in triplicates as previously described.[7,11] Briefly, confluent cells (4-5 day incubation) were cultured for 24 hr in 24-well flat bottom microtiter plates ($\tilde{}$ 5 x 10^5/1 mL/well) and incubated at 37°C in 5% CO_2, 95% air to allow the cells to attach. The medium was then removed and the cells were infected with isolated *T. gondii* in medium with 3% FBS (1 parasite/cell). After 1 hr incubation, the cultures were washed with media with 10% FBS to remove extracellular parasites. FBS was maintained at a final concentration of 10%. Seven concentrations of the compound were then added to cultures of the parasite-infected cells to give a final concentration of 0, 5, 10, 25, and 50 μM. Drugs were dissolved in 50% ethanol to give a final concentration of 2.5% ethanol when added to the wells. After an additional 18 hrs incubation the medium was replaced with 1 mL drug free media containing [5,6-^{13}H]uracil (2 μCi/mL) and incubated for another 6 hrs after which the media was removed. The fibroblasts were released from the wells by trypsinization with addition of 200 μL trypsin/EDTA (2.5X) to each well. After 10 min incubation, 1 mL of ice cold 10% trichloroacetic acid (TCA) was added to each well. The plates were then placed on a shaker to insure the detachment of the cells. The suspended contents of each well was filtered through GF/A 2.4 cm glass microfiber filters (Whatman, Hillsboro, OR0, which were pre-washed each with 1 mL double distilled H_2O and dried. After filtration, the filters were washed with 10 mL methanol, left to dry, then placed in scintillation vials containing 5 mL of Econo-Safe

scintillation fluor (Research Products International Corp., Mount Prospect, IL), and radioactivity was counted using an LS5801 Beckman scintillation counter.

Absence of Toxicity of 6-(Substituted benzylthio)purine Ribosides Analogues to Mammalian Fibroblasts.

Possible toxicity against fibroblast feeder cells by the same doses of the various analogues used in the above experiments was measured, at least in triplicates, using a modification of the Microculture Tetrazolium [MTT] assay on uninfected monolayers of human foreskin fibroblasts (grown for no more than 30 passages) in RPMI 1640 medium.[11,12] Briefly, confluent cells were incubated for at least 24 hr in 96-well flat bottom microtiterplates [~ 10^5/200 μL/well] at 37°C in 5% CO_2, 95% air to allow the cells to attach. The medium was then replaced with 200 μL of fresh medium. The appropriate concentration of the compounds was dissolved in 50 μL of medium, and added to each well to give the desired final concentrations. The cultures were then incubated for 48 hr after which 50 μL of sterile MTT solution [2 mg/1 mL PBS] was added to each well. MTT solution was sterilized by filtration through 0.22 μm filters [Costar, Cambridge, MA]. After 4 hr incubation, the medium was removed and 100 μL of dimethylsulfoxide [DMSO] was added to each well and the plates were shaken gently for 2-3 min to dissolve the formed formazan crystals. The absorbance was measured at 540 nm using a computerized microtiterplate reader [Themomax, Molecular Devices].

References

(1) Gazzinelli, R.T.; Denkers, E.Y.; Sher, A. Host resistance to *Toxoplasma gondii*: Model for studying the selective induction of cell-mediated immunity by intracellular parasites. *Infect Agent Dis*. **1993,** *2*,139-149.

(2) Navia, B.A. Cerebral toxoplasmosis complicating the acquired immune deficiency syndrome: clinical and neuropathological findings in 27 patients. *Ann. Neurol.* **1986**, *19*, 224-238.

(3) Dubey J.P.; Beattie, C.P. Toxoplasmosis of Animals and Man. CRC Press, Boca Raton, FL, **1988.**

(4) Remington, J.S.; McLeond, R.; Desmonts. G. Toxoplasmosis. In: Remington JS, Klein JO, (eds.): *Infectious Diseases of the Fetus and Newborn Infant*. Philadelphia: W.B. Saunders Company, **1995**, p.140-267.

(5) Subauste, C.S.; Remington. J.S. Immunity to *Toxoplasma gondii. Curr. Opin. Immunol.* **1993**, *5*, 532-537.

(6) Krug, E.C.; Marr, J.J.; Berens, R.L. Purine Metabolism in *Toxoplasma gondii*, *J. Biol. Chem*. **1989**, *264*, 10601-10607.

(7) el Kouni, M.H. Potential chemotherapeutic targets in the purine metabolism of parasites. *Pharmacol Therapeut.* **2003**, *99*, 283–309.

(8) Wong, S.; Remington. J.S. Biology of *Toxoplasma gondii*, *AIDS*, **1993**, *7*, 299-316.

(9) Pfefferkorn, E.R.; Pfefferkorn, L.C. The biochemical basis for resistance to adenine arabinoside in a mutant of *Toxoplasma gondii*. *J. Parasitol*. **1978**, *64*, 486-492.

(10) Iltzsch, M. H.; Uber, S.S.; Tankersley, K.O.; el Kouni, M.H. Structure activity relationship for the binding of nucleoside ligands to adenosine kinase from *Toxoplasma gondii*. *Biochem. Pharmacol*. **1995**, *49*, 1501-1512.

(11) el Kouni, M. H.; Guarcello, V.; Al Safarjalani, O. N.; Naguib, F. N. M. Metabolism and selective toxicity of 6-Nitrobenzylinosine in *Toxoplasma gondii*. *Antimicrob. Agents Chemother.* **1999**, *43*, 2437-2443.

(12) Al Safarjalani, O. N.; Naguib, F. N. M. and el Kouni, M. H. Uptake of nitrobenzylthioinosine and purine β-L-nucleosides by intracellular *Toxoplasma gondii. Antimicrob. Agents Chemother.* **2003**, *47*, 3247–3251.

(13) Brajeswar, P.; Chen, M.F.; Paterson, A.R.P. Inhibitors of Nucleoside Transport. A Structure-Activity Study Using Human Erythrocytes. *J. Med. Chem.* **1975**, *18*, 968-973.

(14) (a) Griffith, D. A.; Jarvis, S. M.; Nucleoside and nucleobase transport systems in mammalian cells. *Biochim. Biophys. Acta.* **1996**, *1286*, 153-181. (b) Buolamwini, J. K.; Nucleoside transport inhibitors: Structure-activity relationships and potential therapeutic applications. *Curr Med. Chem.* **1997**, *4*, 35-66. (c) Cass, C. E.; Young, J. D.; Baldwin, S. A.; Cabrita, M. A.; Graham, K. A.; Griffiths, M.; Jennings L. L.; Mackey, J. R.; Ng, A. M.; Ritzel, M. W.; Vickers, M. F.; Yao, S. Y.; Nucleoside transporters of mammalian cells. *Pharmaceutical Biotechnology*, **1999**, *12*, 313-352.

(15) Ceulemans, G.; Busson, R.; Weyns, N.; Vandendriessche, F.; Rozenski, J.; Ijzerman, A; Herdewijn, P. Synthesis of 3'-Fluoro-3'-deoxy-N^6-cyclopentyladenosine; *Nucleosides Nucleotides*, **1994**, *13*, 1991-2000.

(16) Frechet, J.; M.J.; Haque, K.E. Use of polymers as protecting groups in organic synthesis. II. Protection of Primary alcohol functional groups; *Tetrahedron lett.* **1975**, *35*, 3055-3056.

(17) (a) For the synthesis of 2-fluorobenzylmercaptan: Sirakawa, K.; Aki, O.; Tsujikaw, T.; Tsuda, T. S-Alkylthioisothioureas, *Chem. Pharm. Bull.* **1970**, *18*, 235-242 (b) For the synthesis of 3,4-dichlorobenzylmercaptan: Boenigk, J. W.; Christian, J. E.; Jenkins, G. L. Synthesis of certain derivatives of thiols. *J. Am. Pharm. Assoc.*, **1949**, *38*, 357-360. (c) For the synthesis of 4-nitrobenzylmercaptan: Molina, P.; Alajarin, M.; Vilaplana, M. J.; Katritzky, A. R. One pot conversion of alkyl-halides into thiols under mild conditions.

Tetrahedron lett. **1985**, *26*, 469-472 (d) For the synthesis of 4-acetoxybenzylmercaptan: Daines, R.A.; Chambers, P.A.; Eggleston, D.S.; Foley, J.J.; Griswold, D.E.; Haltiwanger, R.C.; Jakas, D.R.; Kingsbury, W.D.; Martin, L.D.; Pendrak, I.; Schmidt, D.B.; Tzimas, M. N.; Sarau, H.M. (E)-3-[[[[6-(2-Carboxyethenyl)-5-[[8-(4-methoxyphenyl)octyl]oxy]-2-pyridinyl]methyl]thio]methyl]benzoic acid and related-compounds - high-affinity leukotriene B-4 receptor antagonists. *J. Med. Chem.* **1994**, *37*, 3327-3336 (e) For the synthesis of 4-bromobenzylmercaptan: Hancock, J.R.; Hardstaff, W.R.; Johns, P.A.; Langler, R.F.; Mantle, W.S. Regiochemistry and reactivity in the chlorination of sulfides. *Can. J. chem.* **1983**, *61*, 1472-1480. (f) For the synthesis of 3-methylbenzylmercaptan: Bacon, R.G.; Guy, R.G. Thiocyanogen chloride .4. Reaction with Aromatic hydrocarbons - heterolytic and homolytic substitution in benzene homologues. *J. Chem. Soc.* **1961**, (Jun), 2428-2435. (g) For the synthesis of 4-cyanobenzylmercaptan and 3-Nitrobenzylmercaptan: Bellas, M.; Tuleen, D. L.; Field, L. Organic disulfides and related substances .22. Substituted benzyl 2-(N-decylamino) ethyl disulfide hydrochlorides. A possible neighboring-group effect involving sulfur. *J. Org. Chem.* **1967**, *32*, 2591-2595. (h) Respective benzylmercaptans for the synthesis of **6a**, **6g**, **6j**, **6m** and **6q** were purchased from Lancaster Synthesis Inc, Windham, NH (i) Respective benzylmercaptans for the synthesis of **6c**, **6k**, **6p** and **6t** were purchased from Aldrich Chemical Co., Inc., Milwaukee, WI (j) Respective benzylmercaptans for the synthesis of **6e**, **6h** and **6r** were purchased from Fluorochem USA, West Columbia, SC.

(18) Bunin, B.A.; *The Combinatorial Index*. San Diego: Academic Press, **1998**, p.55.

(19) (a) Davies, L.P., Baird-Lambert, J.; Marwood, J.F. Studies on several pyrrolo[2,3-*d*]pyrimidine analogues of adenosine which lack significant agonist activity at A1 and A2 receptors but have potent pharmacological activity in vivo. *Biochem. Pharmacol.* **1986**, *35*,

3021-3029. (b)Ugarkar, B.G.; DaRe, J.M.; Kopcho, J.J.; Browne, E.; Schnazer, J.M.; Wiesner, J.B.; Erion, M.D. Adenosine Kinase Inhibitors.1. Synthesis, Enzyme Inhibition, and Antiseizure activity of 5-Iodotubercidin Analogues. *J. Med. Chem.* **2000**, *43*, 2883-2893. (c) Ugarkar, B.G.; Castellino, A.J.; DaRe, J.M.; Kopcho, J.J.; Wiesner, J.B.; Schnazer, J.M.; Erion, M.D. Adenosine Kinase Inhibitors.1. Synthesis, Enzyme Inhibition, and Antiseizure activity of Diaryltubercidin Analogues. *J. Med. Chem.* **2000**, *43*, 2894-2905.

(20) (a) Schumacher, M.A.; Scott, D.M.; Mathews, I.I; Ealick, S.E.; Roos, D.S.; Ullman, B.; Brennan, R.G. Crystal Structure of *Toxoplasma gondii* adenosine kinase reveal a novel catalytic mechanism and prodrug binding, *J. Mol. Biol*. **2000**, *298*, 875-893. (b) Darling, J. A.; Sullivan, W. J.; Carter, D.; Ullman, B.; Roos, D. S.; Recombinant expression, purification, and characterization of *Toxoplasma gondii* adenosine kinase. *Mol Biochem. Parasit.* **1999**, *103*, 15-23.

(21) Chang, G.; Guida, W.C.; Still, W.C. An internal coordinate Monte Carlo method for searching conformational space. *J. Am. Chem. Soc.* **1989**, *111*, 4379-4386.

(22) Guida, W.C.; Bohacek, R.S.; Erion, M.D. Probing the conformational space available to inhibitors in the thermolysin active site using monte carlo/energy minimization techniques. *J. Comput. Chem.* **1992**, *13*, 214-228.

(23) Ealick, S.E.; Babu, Y.S.; Bugg, C.E.; Erion, M.D.; Guida, W.C.; Montgomery, J.A.; Secrist, J.A. Application of crystallographic and modeling methods in the design of purine nucleoside phosphorylase inhibitors. *Proc. Natl. Acad. Sci. USA*. **1991**, *88*, 11540-11544.

(24) Sullivan Jr., W.J.; Chiang, C.W.; Wilson, C.M.; Naguib, F.N.M.; el Kouni, M.H., Donald, R.G.K.; Roos, D.S. Insertional tagging and cloning of at least two loci associated with

resistance to adenine arabinoside in *Toxoplasma gondii*, and cloning of the adenosine kinase locus. *Mol. Biochem. Parasitol*. **1999**, *103*, 1-14.

(25) Bradford, M. M. A rapid and sensitive method for the quantitation of microgram quantities of protein utilizing the principle of protein-dye binding. *Anal. Biochem*. **1976,** *72*, 248-254.

(26) Cha, S. Kinetics of enzyme reactions with competing aternative substrates. *Mol. Pharmacol.* **1968**, *4*, 621-629.

CHAPTER 2

MOLECULAR MECHANISMS OF ADEFOVIR SENSITIVITY AND RESISTANCE IN HBV POLYMERASE MUTANTS: A MOLECULAR DYNAMICS STUDY

Introduction

Although effective vaccines have been available for Hepatitis B virus (HBV) for the past 20 years, chronic infection with HBV is still among the top 10 viral infections.[27] Agents currently available for treatment of HBV can be divided into two groups. The immunomodulators, which include interferon-α thymosin-α1[28] and potential therapeutic vaccines,[29] and nucleoside or nucleotide analogues, among which lamivudine (3TC) and adefovir dipivoxil (hepsera®) have been approved by US FDA and L-FMAU (clevudine), L-dT (telbivudine) and entecavir are undergoing phase III clinical trials. Nucleoside analogues act by suppressing HBV replication at the level of DNA synthesis. Besides their potent antiviral activity, other advantages include oral administration, excellent tolerance, and the possibility of treatment of several subgroups of chronic hepatitis B patients with high risk of side effects after or with contraindications to IFN-α therapy.

The efficacy of IFN-α against HBeAg-positive HBV has been established in numerous studies.[30] However, the overall response rates are low and treatment with IFN-α is associated with substantial dose-limiting adverse effects[31] (depression and influenza-like symptoms). On the other hand, lamivudine (2'3'-dideoxy-3'-thiacytidine;[-]-β-L-isomer), a nucleoside analogue, which was developed for the treatment of HIV (approved by US FDA for HIV infection in 1995), but was also shown to be a potent inhibitor of HBV DNA replication[32] (approved by US FDA for chronic HBV infection in 1998), is effective in reducing serum HBV DNA levels by about 4.0 log10 copies/mL.[33] However, long-term lamivudine treatment for chronic hepatitis B virus (HBV) infection induces the emergence of lamivudine resistant HBV mutant strains. The emergence rate of lamivudine-resistant HBV ranges from 17-46% at 1 year to as high as 67-75% after 3-4 years of continuous therapy.[34] The predominant lamivudine resistant mutations in

HBV-infected patients are rtM204V and rtM204I (C domain) which frequently occur in combination with second mutation, rtL180M (B domain). The clinical frequency of lamivudine-resistant mutants were 18.6% for rtM204I, 1.4% for rtM204V, 11.4% for rtL180M-M204I, and 64.3% for rtL180M-M204V.[35]

The recent addition to NRTI's arsenal against HBV is adefovir dipivoxil. The drug received approval by the US FDA for the use in treatment of chronic HBV infection, in September of 2002. It has demonstrated activity against wild-type and lamivudine resistant strains of HBV. But in contrast to lamivudine therapy, ADV therapy is associated with delayed and infrequent selection of drug resistant viruses.

Recently, after 96 weeks of therapy with adefovir dipivoxil, a novel mutation from asparagine to threonine at residue rt236 in domain D of the HBV polymerase has been reported.[37] In vitro HBV carrying rtN236T mutation displayed reduced susceptibility to ADV, but remained sensitive to lamivudine.[37, 38] This prompted us to study the molecular basis of resistance conferred by this novel mutation on the efficacy of ADV-DP. The work presented here demonstrates the molecular basis of mechanism of ADV-DP against lamivudine-resistant mutants and its decrease in susceptibility for rtN236T HBV polymerase mutant.

Materials and Methods

The three-dimensional structure of HBV polymerase is not yet available, however, its homology model has been reported.[39, 40] Our model was constructed using HIV-1 reverse transcriptase as a template.[40] The two Mg^{2+} ions, thymidine triphosphate and 7/4 (template/primer) duplex were located in the same position as the HIV-1 RT.[41] The heterocyclic moiety of the 5th nucleotide in the template of the 7/4 (template-primer) duplex was modified to the base complementary to the incoming NRTIs. Various mutants of HBV polymerase were generated using mutate command

in biopolymer module of SYBYL 6.7 and were subsequently minimized. For energy minimization studies, Sybyl version 6.7 (Tripos Associates, St. Louis, MO) was used. All the minimization calculations were performed on Silicon Graphics Octane2 workstation. The initial conformation of ADV was constructed by builder module in Spartan 5.1.1 (Wavefunctions, Inc. Irvine, CA), which was geometrically optimized through quantum mechanical *ab initio* calculations using RHF/3-21G* basis. The inhibitor triphosphates were manually docked to the active site of the enzyme. Gästeiger-Hückel charges were given to the enzyme-ligand complex with formal charges (+2) to two Mg atoms in the active site. Then, Kollman-All-Atom charges were loaded to the enzyme site from the biopolymer module. In order to eliminate the local strains resulting from merging nucleotides and/or point mutations, residues inside 6Å from the mutated residues and merged nucleotides were annealed until energy change from one iteration to the next was less than 0.05 kcal/mol. The annealed enzyme-inhibitor complexes were further minimized by using Kollman-All-Atom Force Field until the iteration number reached 5,000 or the energy difference from one iteration to the next is less than 0.0001 kcal/mol.[40]

The minimization results were further confirmed by performing molecular dynamics simulations on modeled ternary complex using molecular graphics and simulation program MacroModel, version 8.5 (Schrödinger, Inc). Molecular dynamics simulations on HBV pol. (Wild Type, rt-Leu180Met, rt-Met204Val, rt-Met204Ile, rt-Leu180Met & rt-Met204Val, rt-Leu180Met & rt-Met204Ile and rt-Asn236Thr) – DNA – Nucleotide (dATP, ADV–DP) were performed with MMFFs force field in the presence of GB/SA continuum water model on a Silicon Graphics Tezro workstation running IRIX 6.5 operating system. Dynamics simulations were carried out by heating the system from 0 to 300K over 5ps and equilibrating at 300K for an additional 10ps. Production dynamics simulations were carried out for 500ps with a step size of

1.5fs at 300K. A shake algorithm was used to constrain covalent bonds to hydrogen atoms. For dynamics calculations, the residues further away than 15Å from the active site were not considered and the residues from 6 to 15 Å were constrained by harmonic constraints. Only residues inside the 6Å sphere from the nucleotide were allowed to move freely.

Results & Discussion

In wild type HBV polymerase, 3TC-TP makes favorable van der Waals contact with Met204. However, rtM204V HBV polymerase mutation causes the movement of 3TC-TP toward Val204 in order to maintain the favorable van der Waals contact. Movement of 3TC-TP towards the Val204 results in the disruption of the active site geometry.[42] Thus, the rtM204V HBV pol. mutation discriminates the oxathiolane ring of lamivudine at the level of incorporation by disruption of the active site (coordination geometry of Mg^{2+}), which is well correlated with the observed decrease in efficacy of the 3TC in M204V/I mutant.[42]

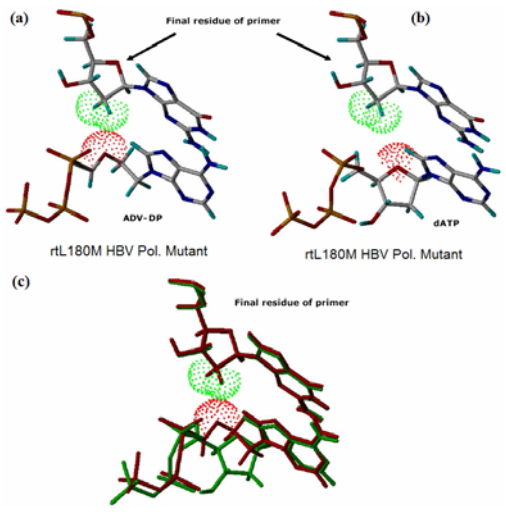

Figure 2.1. (a & b) Binding mode of natural substrate (dATP) and ADV-DP in rtL180M mutant HBV Pol. is shown here along with the van der Waals radii of 4'-oxygen and 2'-hydrogens. (c) dATP and ADV-DP are superimposed onto each other to see the difference in their binding mode.

In rtL180M HBV pol. mutant, the substitution of leucine with methionine (not shown in Figure 2.1 for the sake of clarity) changes the binding mode of ADV-DP slightly by pushing the ADV-DP towards the sugar moiety of the final residue of primer strand (2.1a). This is because methionine side chain is much longer than isoleucine and it extends around the ADV-DP. In order to maintain the proper van der Waals interaction and to avoid any steric clash with the mutated methonine side chain, ADV-DP moves towards the 204 region (Figure 2.1a). In the case of natural substrate (dATP), the 4'-oxygen atom of the sugar moiety doesn't make van der Waals contact with the 2'-hydrogens of sugar moiety of the final residue of the primer strand (Figure 2.1b). But, in the case of ADV-DP, the 4'-oxygen atom makes significant van der Waals contact with the 2'-hydrogens of sugar moiety of the final residue of primer strand (Figure 2.1a). This results in enhanced binding affinity of ADV-DP toward the rtL180M mutant.

In the wild type HBV pol., Met204 doesn't make significant van der Waals contact with the acyclic moiety of ADV-DP (Figure 2.2b). Mutation rtM204V fills the gap between Val204 and the acyclic moiety of ADV-DP and the sugar moiety of the final residue of the primer strand, thereby causing extensive van der Waals interactions (Figure 2.2a). A similar pattern is observed with the rtM204I HBV pol. mutant. Mutation M204I fills this gap better, resulting in increased favorable van der Waals interactions (Figure 2.2c).

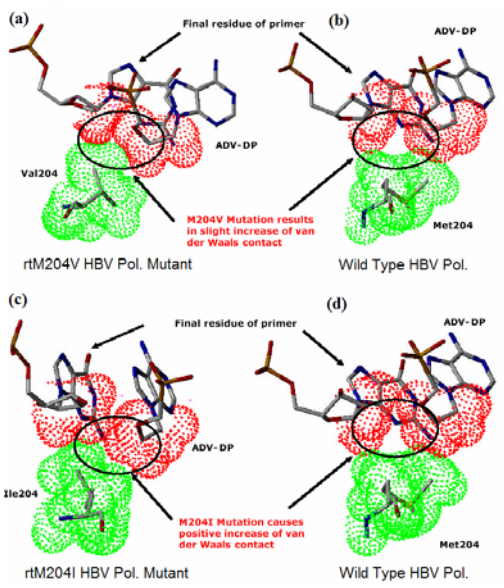

Figure 2.2. (a & b) Binding mode of ADV-DP in rtM204V mutant and wild type HBV pol. (c & d) Binding mode of ADV-DP in rt M204I and wild type HBV pol. is shown.

Binding mode of ADV-DP in double mutants (rtL180M-rtM204V and rtL180M-rtM204I) is same as that observed in single mutations, rtL180M or rtM204V. Since both these mutations are located in different domains of HBV pol. it wasn't possible to show these effects in single graphic. Both these mutations result in increase in van der Waals interaction between ADV-DP, the final residue of the primer strand and the surrounding residues (as observed in individual single point mutations).

In literature,[39, 43] a range of fold increase (FI) values have been reported for these double mutants. In these studies, ADV-DP was found to be more active against double mutants when compared to single point mutants.[39, 43] Our calculations also predict the efficacy of ADV-DP in these double mutants to be better than that in single point mutants. The decreasing order of binding affinity of ADV-DP in these mutants from our studies is: rtL180M-rtM204I > rtL180M-

rtM204V > rtM204I > rtM204V ≈ rtL180M > WT > rtN236T (Table 2.1)

Table 2.1. Correlation between E_{rel} and IC_{50} (Molecular Dynamics Studies)

HBV Polymerase	dATP	ADV-DP		
	Enzyme-DNA-dATP complex[a]	**Enzyme-DNA-ADV-DP complex**[a]	**ΔE_{rel}**[a]	**Fold Increase**[b] **(FI)**
WT	-8521	-8662	-141	1.0
rtL180M	-8467	-8645	-178 (-124)	0.7
rtM204V	-8458	-8638	-180 (-117)	0.7
rtM204I	-8449	-8657	-208 (-136)	0.5
rtL180M - rtM204V	-8396	-8623	-227 (-102)	0.2-0.8
rtL180M - rtM204I	-8389	-8633	-244 (-112)	0.2-1.8
rtN236T	-8516	-8548	-32(-27)	4.4[c]

[a]ΔE_{rel}= (Enzyme-DNA-ADVDP complex) – (Mutant-HBV-DNA-dATP complex) , in kcal/mol, Values in parenthesis are (Enzyme-DNA-ADVDP complex) – (WT-HBV-DNA-dATP complex) ; [b] reference 39 & 43a; [c] reference 43b

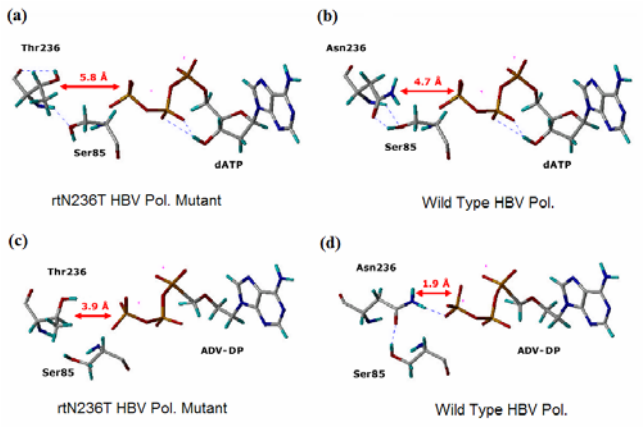

Figure 2.3. (a & b) Binding mode of dATP in rtN236T mutant and wild type is shown here. Notice the distance between the γ-phosphate and residue at rt236 position. (c & d) Binding mode of ADV-DP in rtN236T mutant and wild type is shown here.

As can be seen in Figure 2.3a & 2.3b, rtN236T mutation doesn't change the binding mode and binding geometry of natural substrate significantly. It also doesn't change the net binding affinity of natural substrate (dATP) (Table 2.1), even though it loses one hydrogen bond with Ser85 (Figure 2.3a & 2.3b), but it gains another one between the hydroxy group of Thr236 and the amide backbone (Figure 2.3a). Hence, no significant change in the binding affinity of dATP for WT and rtN236T mutant HBV pol. is observed (Table 2.1). However, for ADV-DP, in wild type HBV pol., one hydrogen bond is between the terminal hydrogen of the Asn236 and the oxygen atom of the γ-phosphate of ADV-DP (Figure 2.3d). The second hydrogen bond is between the carbonyl of the Asn236 and the hydroxy group of the Ser85 (Figure 2.3d). The loss of these two hydrogen bonds (Figure 2.3c) accompanied by significant loss of favorable electrostatic interactions (Table 2.1), results in decreased binding affinity of ADV-DP toward the rtN236T mutant. On comparing the binding mode of dATP and ADV-DP from Figure 2.3, the role of Asn236 in stabilizing the γ-phosphate of ADV-DP becomes evident. Asn236 plays an important

role in stabilizing the γ-phosphate of ADV-DP, which is further confirmed by comparing the relative binding energy of dATP toward WT HBV pol. and rtN236T HBV pol. mutant (Table 2.1).

Conclusions

In summary, from our molecular dynamics studies, we have demonstrated that rtN236T HBV pol. mutation is the true ADV-DP mutation, in a sense that, this mutation doesn't affect the binding affinity of natural substrate (dATP) significantly, but it decreases the binding affinity of ADV-DP towards rtN236T HBV pol. drastically. Lamivudine resistant mutations (rtM204V and rtM204I) results in increased van der Waals contacts between ADV-DP and mutated residues, which accounts for the better binding affinity of ADV-DP towards these mutants. The second lamivudine associated mutation (rtL180M) also results in increase in van der Waals contacts between ADV-DP and the final residue of the primer strand, which accounts for the better binding affinity of ADV-DP in these mutants. The observed increase in efficacy of ADV-DP is not only because of the enhanced binding affinity of ADV-DP towards these mutants (rtM204V, rtM204I, rtL180M, rtL180M-M204V/I180M), but also is supplemented by the decreased affinity of the natural substrate (dATP) towards these lamivudine-resistant mutants.

References

(27) Lee, W. M. N. Engl. J. Med. 1997, 337, 1733-45

(28) Chien, R. N.; Liaw, Y. F.; Chen, T. C.; Yeh, C. T.; Sheen, I. S. Hepatology, 1998, 27, 1383-87

(29) Michel, M. L.; Pol, S.; Brechot, C.; Tiollais, P. Vaccine, 2001, 19, 2395-99

(30) Wong, D. K.; Cheung, A. M.; O'Rourke, K.; Naylor, C. D.; Detsky, A. S.; Heathcote, J. Annals of Internal Medicine 1993, 119, 312-23.

(31) Vinayek, R.; Shakil, O. Viral Hep. Rev. 1997, 3, 167-177.

(32) Doong, S.; Tsai, C.; Schinazi, R. Proc. Natl. Acad. Sci. USA 1991, 88, 8495-99.

(33) Honkoop, P.; de Man, R. A.; Niesters, H. G.; Main, J.; Nevens, F.; Thomas, H. C.; Fevery, J.; Tyrrell, D. L.; Schalm, S. W. J. Viral Hepat. 1998, 5, 307-12.

(34) (a) Lai, C. L. N. Engl. J. Med. 1998, 339, 61-8. (b) Bartholomeusz, A.; Schinazi, R. F.; Locarnini, S. A. Viral Hepatitis Reviews, 1998, 4, 167-87.

(35) (a) Allen, M. L.; Deslauriers, M.; Andrews, C. W.; Tipples, G. A.; Walters, K. A.; Tyrrell, D. L. J.; Brown, N.; Condreay, L. D. Hepatology, 1998, 27, 1670-77. (b) Banhamou, Y.; Bochet, M.; Thibault, B.; Martino, V. D.; Caumes, E.; Bricaire F.; Opolon, P.; Katlama, C.; Poynard, T. Hepatology, 1999, 30, 1302-06

(36) Xiong, X.; Flores, C.; Yang, H.; Toole, J. J.; Gibbs, C. S. Hepatology, 1998, 1669-73.

(37) Aloman, C.; Wands, J. R. Hepatology, 2003, 38, 1584-87.

(38) Dando, T. M.; Plosker, G. L. Drugs, 2003, 63, 2215-34.

(39) Das, K.; Xiong, X.; Yang, H.; Westland, C. E.; Gibbs, C. S.; Sarafianos, S. G.; Arnold, E. J. Virology, 2001, 75, 4771-4779.

(40) Chong, Y.; Chu, C. K. Bioorg. Med. Chem. Letts. 2002, 12, 3459-62.

(41) Huang, H.; Chopra, R.; Verdine, G. L.; Harrison, S. C. Science 1998, 282, 1669-75.

(42) Chong, Y.; Stuyver, L.; Otto, M. J.; Schinazi, R. F., Chu, C. K. Antivir. Chem. chemother. 2003, 14, 309-19.

(43) (a) Locarnini. S. J. Hepatology, 2003, 39, S124- 32. (b) Villeneuve, J. P.; Durantel, D.; Durantel, S.; Westland, C.; Xiong, S.; Brosgart, C. S.; Gibbs, C. S.; Parvaz, P.; Werle, B.; Trepo, C.; Zoulim, F. J. Hepatology, 2003, 39, 1085-89.